SCIENTIFIC REPORTS
nature research

OPEN

Computational translation of drug effects from animal experiments to human ventricular myocytes

Aslak Tveito[1]✉, Karoline Horgmo Jæger[1], Mary M. Maleckar[1], Wayne R. Giles[2] & Samuel Wall[1]

Using animal cells and tissues as precise measuring devices for developing new drugs presents a long-standing challenge for the pharmaceutical industry. Despite the very significant resources that continue to be dedicated to animal testing of new compounds, only qualitative results can be obtained. This often results in both false positives and false negatives. Here, we show how the effect of drugs applied to animal ventricular myocytes can be translated, quantitatively, to estimate a number of different effects of the same drug on human cardiomyocytes. We illustrate and validate our methodology by translating, from animal to human, the effect of dofetilide applied to dog cardiomyocytes, the effect of E-4031 applied to zebrafish cardiomyocytes, and, finally, the effect of sotalol applied to rabbit cardiomyocytes. In all cases, the accuracy of our quantitative estimates are demonstrated. Our computations reveal that, in principle, electrophysiological data from testing using animal ventricular myocytes, can give precise, quantitative estimates of the effect of new compounds on human cardiomyocytes.

Our main goal was to develop model-based methods evaluating whether measurements of drug effects on animal cardiomyocytes can be translated to corresponding drug effects on human cardiomyocytes. The analysis reveals how effects on membrane currents carried by the same ion channel protein in animal and humans can be translated in order to evaluate and understand human ventricular action potentials. This approach provides a framework revealing unwanted side effects early in the development of novel drug candidates. The usefulness of animal models in understanding human electrophysiology is unquestioned, but limited by the inherent difference between the human and animal action potentials; see e.g.[1–3]. Often, this gives rise to difficulties in direct translation; even if some of the ion channels involved are functionally nearly identical, the overall composition of membrane ion channels can differ substantially between species. Therefore, block of the same ion channel in two different species may yield very different perturbations of the respective action potentials.

This limitation has serious implications for the overall efficiency and effectiveness of drug development. Currently, this process takes 10 to 15 years, with an average cost of ~2.5 billion USD[4]. Preclinical development, including animal testing for safety predictions, accounts for ~60% of these costs[5]. However, despite this cost and effort, many promising candidate drugs exhibit toxicity that has not been predicted prior to clinical trials and, ultimately, emerging therapies[6]; clearly, more quantitatively predictive tools are needed. Assuming that the major currents underlying the ventricular action potential are governed by the same or similar ion channel alpha subunit in an animal and in a human heart cell, and that these proteins have comparable function and are relatively well understood[1,7–11], our approach can be used to translate measured pharmacological effects on the action potential in animal models to those in healthy human adult cardiomyocytes.

Previously[12,13], we have developed a theoretical approach which allowed translation of measurements obtained on human induced pluripotent stem cell-derived cardiomyocytes (hiPSC-CMs) to adult cardiomyocytes. In brief, we have demonstrated that after inverting hiPSC-CM data, and finding the effect of a drug candidate on every ion channel, these findings can be accurately mapped to the case of mature cardiomyocytes. Thus, the effect of the drug on adult human heart cells can be deduced from measurements of hiPSC-CMs. Our aim here is to show that a similar approach can be employed in translation from animal myocytes to human results.

In order to fully translate the effect of a drug from data obtained from either hiPSC-CMs or animals, the effect of the drug must be used to estimate parameters of the associated mathematical model. This is indeed a challenging process; see e.g.[14–16] with significant uncertainty. Here, in order to focus on the trans-species mapping, we

[1]Simula Research Laboratory, Fornebu, Norway. [2]Department of Physiology and Pharmacology, Faculty of Medicine, University of Calgary, Calgary, Canada. ✉e-mail: aslak@simula.no

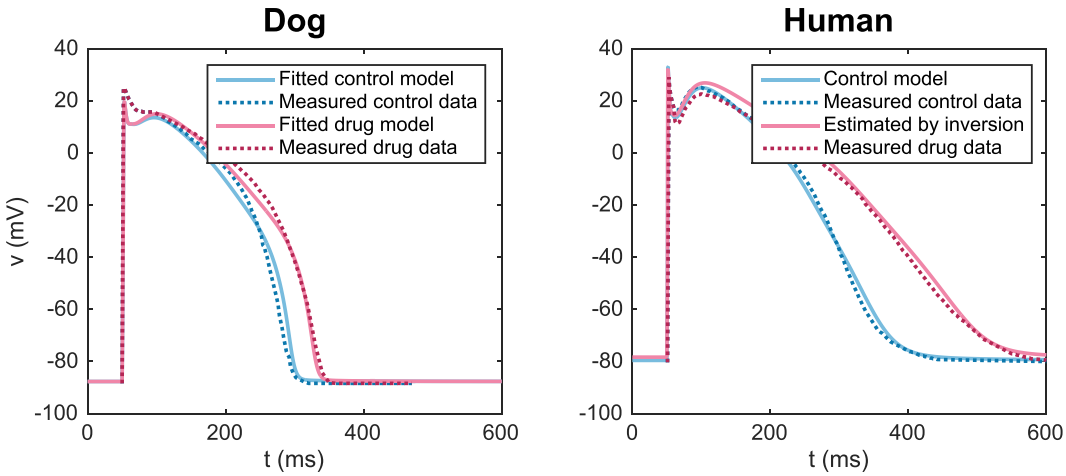

Figure 1. Dog (left) and human (right) ventricular action potentials in the control case and in the presence of 50 nM of the I_{Kr} blocker dofetilide. The dotted lines show measured data from[7], and solid lines show simulation results. Note that the drug effect used in the simulation of the human AP was estimated from the dog data.

	Dog, control measured	Dog, drug measured	Human, control measured	Human, drug measured	Human, control model	Human, drug estimated based on dog data
APD50 (ms)	201	+17.5%	230	+33.3%	221	+38.0%
APD90 (ms)	239	+18.3%	312	+44.3%	317	+40.2%

Table 1. APD values computed from measured and simulated action potentials in the control case and in the presence of 50 nM of the I_{Kr} blocker dofetilide. The cells in both the experiments[7] and in the mathematical model were paced at 1 Hz.

use the techniques developed in[13], simplified considerably by assuming that we know which of the ion channels that are affected by a given drug. In this simplified case it is sufficient to only have data on the transmembrane potential.

Results

Here, we demonstrate that it is possible to estimate the effect of a drug candidate on humans solely based on measurements of analogous effects on animal cardiomyocytes. The dog data presented in[7] is employed together with our method to estimate the effect that dofetilide will have on humans. Also, in[7], the effect of dofetilide on human cardiomyocytes was reported, allowing us to assess the quality of our estimates. Additionally, we used the data provided in[17] on zebrafish to estimate the effect of the drug E-4031 on humans. While the effect on human cardiomyocytes is not reported in[17], this has been reported in[18,19], which we again used to assess the accuracy of our estimates. Finally, we used rabbit data presented in[20] to estimate the effect of sotalol on human myocytes; data on human cardiomyocytes in response to sotalol has been presented in[20,21] and is used here for comparison and assessment.

Quantitative translation from dog to human. In Fig. 1, our method (see below) is applied to data published in[7]. In the left panel, experimental data (dotted) is shown for control (blue) and when 50 nM of the I_{Kr} blocker dofetilide is applied (red) to canine myocytes. Solid lines show the results of the mathematical model (Supplementary Information). The parameters defining a control model and an IC_{50} value representing the effect of the drug are estimated and used to model the no drug case (solid blue line) and when the drug has been applied (solid red line).

In the right panel, the control data (dotted blue) and the control mathematical model (solid blue) are illustrated for the human ventricular myocyte. We used the method to estimate the effect of the I_{Kr} blocker on the ventricular AP model of the dog, and this effect is translated (Supplementary Information) to the human AP model; this estimated AP (solid red) fits the measured data from[7] very well.

In Table 1, we compare selected biomarkers (APD50 and APD90) for the control case of dog cardiomyocytes (measured), dog cardiomyocytes subjected to the drug (measured), the human control (measured), the human control (model), human cardiomyocytes subjected to the drug (measured) and human cardiomyocytes subjected to the drug (estimated as based on the dog data, as described in the Supplementary Information). All experimental data are taken from[7]. For the dog data, the APD50 is increased by 17.5% when the drug is added while, for human cells, the measured increase in APD50 is 33.3%. When we compare the output from the mathematical model for the control case, and the one where the effect of the drug is added to the model, we observe an increase

	Zebrafish control measured	Zebrafish drug measured	Human control measured	Human drug measured	Human control model	Human drug, estimated based on zebrafish data
APD50 (ms)	108	+38.7%	255 (B)	+27.7% (B)	221	+58.0%
				+54.2% (J)		
APD90 (ms)	144	+24.1%	356 (B)	+31.2% (B)	317	+62.8%
				+65.1% (J)		

Table 2. APD values computed from measured and simulated action potentials in the control case and in the presence of 1 μM of the I_{Kr} blocker E-4031. The zebrafish data is from[17] and the human data is from Bussek *et al.*[18] (B) and Jost *et al.*[19] (J).

	Rabbit, control measured	Rabbit, drug measured	Human, control measured	Human, drug measured	Human, control model	Human, drug estimated based on rabbit data
APD50 (ms)	162	+21.2% (10 μM)	185 (B)	+32.3% (30 μM) (B)	221	+24.7% (30 μM)
		+54.3% (52 μM)	233 (O)	+20.6% (30 μM) (O)		
APD90 (ms)	194	+19.6% (10 μM)	235 (B)	+37.5% (30 μM) (B)	317	+28.8% (30 μM)
		+54.1% (52 μM)	302 (O)	+28.2% (30 μM) (O)		

Table 3. Selected APD values from experimental and simulated action potentials in the control case and in the presence of the I_{Kr} blocker sotalol. The rabbit experimental data is taken from[20], and includes the two drug doses 10 μM and 52 μM. The human experimental data is taken from Baczkó *et al.*[20] (B) and Orvos *et al.*[21] (O) and is measured for the drug dose of 30 μM.

of 38.0%. Thus, based only on data from the dog, our estimate of the increase of the APD50 for humans differs little from the measured value (38.0 vs 33.3%). The analysis of the APD90 also reveal a similarly small difference (40.2 vs. 44.3%). We conclude that the dog data on APD50/APD90 can be used to estimate the effect of the I_{Kr} blocker dofetilide on human cardiomyocytes well. Furthermore, the mathematical model estimates an IC_{50} value of 17 nM for block of I_{Kr} by dofetilide. This value is in good agreement with IC_{50} values for I_{Kr} block by dofetilide found in literature (1–70 nM[21–24]).

Quantitative translation from zebrafish to human. In Table 2, the same method was applied to data from zebrafish cardiomyocytes[17]. Again, we have focused on experimental APD50 and APD90 values for zebrafish in the control case and the increase caused by the application of 1 μM of the I_{Kr} blocker E-4031. In addition, we report the increases in APD50/APD90 from measurements of human cardiomyocytes exposed to 1 μM E-4031 from Bussek *et al.*[18] (B) and Jost *et al.*[19] (J).

Finally, we report the increases in APD50 and APD90 estimated for human cardiomyocytes as based on the measurements of zebrafish cardiomyocytes. Again, we observe that the APD changes estimated using the mathematical model for the human case agree well with the measured effects for human cells. For APD50, our method estimates a 58.0% increase, while the increase is 27.7% (B) or 54.2% (J) in the experimental data. Similarly, the method estimates a 62.8% increase of APD90, while the experimental data reports a 31.2% (B) or 65.1% (J) increase. Furthermore, the method estimates an IC_{50} value of 44 nM for block of I_{Kr} by E-4031, in line with corresponding IC_{50} values found in literature (10–397 nM[25–30]).

Quantitative translation from rabbit to human. Table 3 shows the result when the same method is applied to rabbit ventricular myocyte data from[20]. In this case, two doses (10 μM and 52 μM) of the I_{Kr} and I_{CaL} blocker sotalol were employed. In addition[20,21], provide measured data for human cardiomyocytes exposed to 30 μM sotalol. The column at the extreme right in Table 3 reports the increases in human APD50 and APD90 estimated based on the rabbit data. Both the estimated increase in APD50 (24.7%) and APD90 (28.8%) seem to be in good agreement with the measured human values from[20,21] (32.3% and 20.6% for APD50 and 37.5% and 28.2% for APD90). The method estimates an IC_{50} value of 12 μM for block of I_{Kr} by sotalol and an IC_{50} value of 102 μM for block of I_{CaL}. The corresponding IC_{50} values found in literature are 51–343 μM for I_{Kr}[21–24] and 193 μM for I_{CaL}[23].

Discussion

The use of animal models to aid in understanding of human anatomy and physiology is centuries old, see e.g.[31,32].

In the case of the electrophysiology of the vertebrate heart, this type of comparative study[33] has led to deep insight into key physiological mechanisms, but it has been difficult to use these models quantitatively due to inherent species differences. More specifically, while animal cells are routinely used as part of drug development, their quantitative usefulness is hampered by the significant differences in human and animal action potential waveforms. At present, the most useful results are obtained by utilizing observed correlations between human and

animal biomarkers (see e.g.[34–38]). However, no mechanistic relationship has, to date, been derived to examine how drug candidates may affect human and animal cardiomyocytes differentially. This limits the predictive insights into the therapeutic or toxic effects on humans. In this study, we have shown how an antiarrhythmic drug effect on human ventricular myocytes can be revealed solely by measuring an analogous effect of the drug on animal ventricular myocytes. This new investigative capability opens a wide variety of possibilities to improve the testing of novel compounds.

Initially, we have shown that canine data can be used to reliably predict the effect of the drug dofetilide on human myocytes as judged by changes in the common biomarkers APD50 and APD90. Similarly, data from zebrafish action potentials was used to estimate the effect of E-4031 on human ventricular myocytes. Finally, the effect of sotalol on rabbit cardiomyocytes was used to estimate the effect of the same drug on human ventricular myocytes, and the results were revealing.

Our method can only be used to estimate a selected drug effect on ion currents that have significant impact on both the animal and the human action potentials. If one current is very small in an animal but very large in a human, drug effects on that current cannot be estimated using the present technique. One such case is illustrated in Fig. 1 of[1], where the action potential of human, canine, rabbit, guinea pig and mouse are illustrated together with associated currents. The substantial differences between the human and mouse action potentials and underlying ion currents suggest that it is difficult to use our method to predict the effect of drugs on human cardiomyocytes by measuring the effect of the drug on mouse cardiomyocytes.

In the present study, our principal aim was to generalize the methods we have developed previously[12,13] for extrapolating drug effects obtained using hiPSC-CMs to healthy, mature human ventricular myocytes. Importantly, we found that the an equivalent approach can be used to translate measured pharmacological effects on the action potential in animal models to those in healthy adult human myocytes by employing the same models for the same currents in different cell types. The assumption underlying this approach is that major currents are carried by the same or similar ion channels for which isoforms differences have been measured and are relatively well understood. This is indeed often the case. While sarcolemmal voltage gated ion channels are complex transmembrane proteins of several classes, often composed of more than one interacting or modifying subunit, the alpha subunit of cardiac sodium, potassium, and calcium channels do show very strong primary sequence similarities across species; genome comparisons highlight a number of highly conserved channel families including Nav, Kv, and Cav[39]. For instance, in epicardial adult ventricular myocytes, channels underpinning late repolarization (delayed rectifier currents rapid and slow, I_{Kr}/hERG and I_{Ks}/KvLQT-minK, respectively) are conserved among human, canine, guinea pig, and rabbit cells[8,40]. Again, the transient outward current, I_{to}, prominent in early depolarization in the rabbit ventricle via Kv1.4/4.2/4.3, is similar in presentation and action potential effects in adult human myocytes, as carried by Kv4.3[9]. The inward rectifying K^+ current (I_{Kl}), the L-type Ca^{2+} current (I_{CaL}), and the Na^+/K^+ pump current (I_{NaK}) are also present and effectual in rabbit[10] in addition to other species, as in human. Rabbit measurements of calcium handling and excitation-contraction coupling have long been used as a basis to study and model these important phenomenon in human myocytes[11], and the molecular constituents of all three major depolarizing sarcolemmal currents, I_{CaL}, I_{Na}, and I_{NaCa}, are thought to be relatively consistent across species[1]. To say that conserved sequences implied conservation of overall structure or indeed ion channel function in all cases would be an oversimplification, as differences have been confirmed e.g.[41,42]. However, the relative conservation of expressed ion channel proteins across mammalian species provides a solid basis for application of our methodology for translation of drug effects between species, given an understanding of the divergence, as well as sufficient data for parameterization and validation.

Methods

Mathematical models of the membrane potential of excitable cells are written on the form

$$\frac{dv}{dt} = -\sum_x I_x, \tag{1}$$

see e.g.[43–46]. Here, v is the membrane potential (in mV), t denotes time (in ms) and I_x are the membrane currents (in A/F). Each individual current can be written on the form

$$I_x = \frac{N_x}{AC_m} g_0^x o_x (v - E_x), \tag{2}$$

where A is the area of the cell membrane (in μm^2) and C_m is the specific capacitance of the cell membrane (in $pF/\mu m^2$); both A and C_m are common parameters for every currents in a given type of cardiomyocyte. Furthermore, N_x is the number of channels of type x, g_0^x is the conductance of a single open channel (in nS), o_x is the unitless open probability of the channel. Finally, E_x is the electrochemical equilibrium potential of the channel (in mV). By introducing the constant

$$\rho_x = \frac{N_x}{AC_m}, \tag{3}$$

we get the simpler expression

$$I_x = \rho_x g_0^x o_x (v - E_x). \tag{4}$$

In (4) it is important to note that the characteristics of the dynamics of the specific ion channel under consideration is given by the open probability o_x; the rest of the expression is either constants or the common term

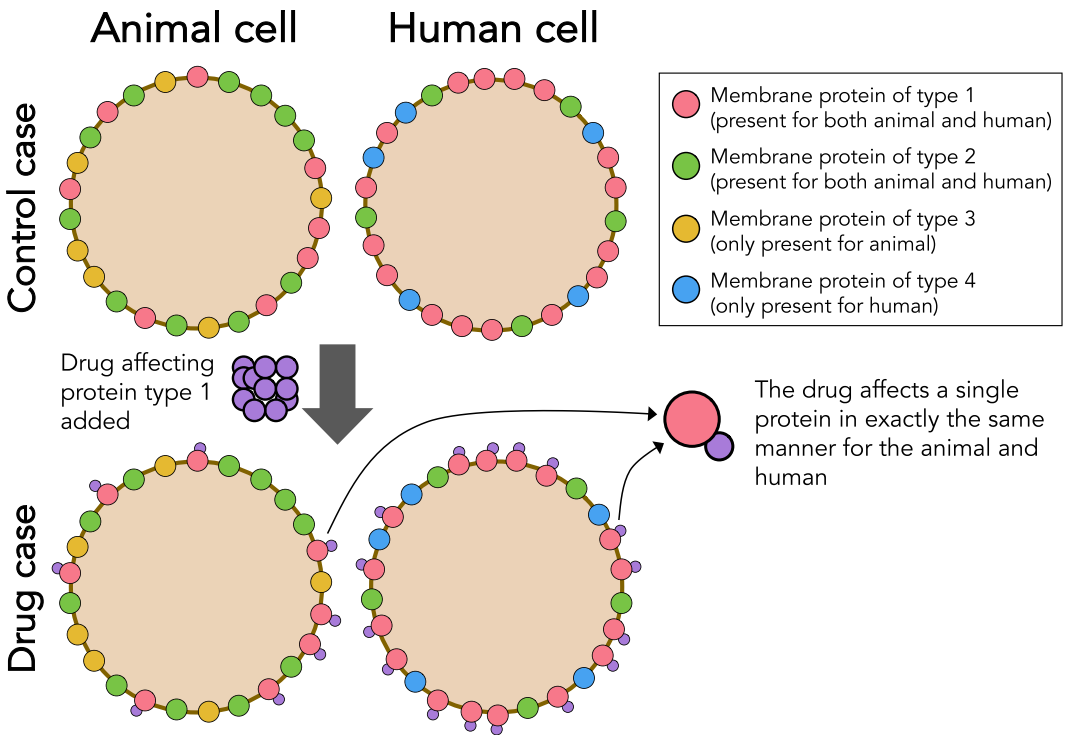

Figure 2. Upper left; illustration of an animal cardiomyocyte that express three types of ion-channels (proteins) in the myocyte membrane surface (sarcolemma). Two of the proteins are also present in the membrane of the human cardiomyocyte (upper right). Note that the human ventricular myocyte also express an additional type of protein *not present* in the animal cell. In the lower panels, both the animal and the human cardiomyocytes are subjected to a blocking drug that binds to one of the protein types. An essential assumption for allowing quantitative translation of animal measurements to estimates of the effect of human cells is that, at the level of a single protein, the effect of the drug is independent of whether the protein is expressed in human or an animal cell membrane.

$(v - E_x)$. The dynamics of o_x can be modelled using a Markov scheme (see e.g.[43,44,47]). Here, it is critical to acknowledge that if the ion channel in two different species are identical, then so is the Markov model governing their dynamics. The diagram in Fig. 2 illustrates the assumptions underlying the translation from animal to human.

The effect of a specific channel blocker is often expressed in terms of an IC_{50} value (see e.g.[48]; here we use the Hill coefficient 1). The IC_{50} value indicates the concentration that reduces the channel conductance by 50%. We assume that when a channel blocker is applied, the current takes the form

$$I_x(D) = \rho_x g_x^0(D) o_x (v - E_x), \tag{5}$$

where we have defined the conductance of the single channel to be

$$g_x^0(D) = \frac{g_0^x}{1 + \varepsilon_x D}. \tag{6}$$

In (6), we have introduced the parameter $\varepsilon_x = 1/IC_{50}$; here D is the drug concentration given in the same unit as the IC_{50} (often μM). Clearly, $I_x(IC_{50}) = \frac{1}{2} I_x(0)$, where $I_x(0)$ is the current in baseline or control case. Note from (5) that we assume that the blocker only affects the maximum conductance of the single channel. This is a known oversimplification since the effects of drugs may be much more complex; see e.g.[47,49,50]. However, this assumption greatly simplifies the identification of the drug effect from measurements, and it is sufficient for our purposes.

IC50 for animal current = IC50 for human current. When a drug effect on an ion channel in an animal myocyte is detected, the key observation for translation to humans is that, given the assumption of functional invariance of channels between species (see Fig. 2), the effect of the drug on a single channel protein must be the same whether the protein is expressed in an animal or human. More specifically, if a current in an animal cardiomyocyte is given by

$$I_A = \rho_A g_0 o (v - E), \tag{7}$$

then the associated human current is given by

$$I_H = \rho_H g_0 o(v - E). \tag{8}$$

If a drug is added to the animal channel with a given IC_{50} value, then, as above, g_0 of (7) is replaced by

$$g^0(D) = \frac{g_0}{1 + \varepsilon D}, \tag{9}$$

where $\varepsilon = 1/IC_{50}$. But since the conductance of the single channel is the same for the animal current and the human current, the single channel conductance of the human model (8) is also replaced by the expression given in (9). Hence, when a drug of concentration D is added we have the currents

$$I_A(D) = \rho_A \frac{g_0}{1 + \varepsilon D} o(v - E), \tag{10}$$

$$I_H(D) = \rho_H \frac{g_0}{1 + \varepsilon D} o(v - E). \tag{11}$$

Therefore, $I_A(IC_{50}) = \frac{1}{2} I_A(0)$, and, similarly, $I_H(IC_{50}) = \frac{1}{2} I_H(0)$, and thus the IC_{50} value of the animal and human current is the same. In principle, this key observation also is valid when the drug effect is modeled as a part of a complex Markov model, since the effect of the drug, on the single channel, again would be the same for animals and humans as long as the single ion channels are identical.

Details regarding the specific choice of action potential model used in our computations and the method used to identify drug effects on single ion channels from membrane potential measurements are given in the Supplementary information.

Supplementary Information

Translating from animal to human. Let us consider a very simple situation where we assume that both the animal myocyte action potential (a) and the human action potential (h) are generated by only two currents. The mathematical models takes then the form

$$\frac{dv^y}{dt} = -\rho_1^y \frac{g_0^1}{1 + \varepsilon_1 D} o_1^y (v^y - E_1) - \rho_2^y \frac{g_0^2}{1 + \varepsilon_2 D} o_2^y (v^y - E_2), \tag{12}$$

where y is either a for animal or h for human. Here, clearly ρ_1^y, ρ_2^y are different for $y = a$ and $y = h$ due to differences in the ion channel density. However, since the ion channels are the same, the Markov model governing the o_1^y, for $y = a$ and $y = h$ are the same.

Suppose now that we have measured an animal dataset sufficient to determine the coefficients ε_1 and ε_2. We immediately observe that we have a complete mathematical model for both the animal and the human action potentials. Using these principles, we can compute the biomarkers of interest for the human case.

Certainly, mathematical models used to represent action potentials are much more complex than the template model given by (12) in the main text; see e.g.[11,51,52]. In our computations, we use the Base model developed in[13], as it systematically uses the same model for the identical ion channel in two different species. Note that in[13] the results of the Base model is compared to the results of the Paci model (for immature cells) and to the Grandi *et al.* model and the ORd model (adult human cells).

Example. In order to explain and illustrate how it is possible to use animal data to gain quantitative insight concerning effects on human ventricular myocytes, we will present a very simple example. Let us for the sake of argument assume that an animal myocyte action potential is governed by

$$\frac{dv}{dt} = -g_1 \mathrm{I}_{\mathrm{Na}} - g_2 \mathrm{I}_{\mathrm{CaL}} - g_3 \mathrm{I}_{\mathrm{Ks}}$$

and the analogous human AP is governed by the very simple model,

$$\frac{dv}{dt} = -k_1 \mathrm{I}_{\mathrm{Na}} - k_2 \mathrm{I}_{\mathrm{CaL}} - k_3 \mathrm{I}_{\mathrm{Kr}}.$$

Here $g_1, g_2, g_3, k_1, k_2, k_3$ are conductances and we assume that they are of significant magnitude. Suppose, for instance, that a drug is applied to the animal ventricular myocytes and inversion of the measured data suggests that the drug is a calcium blocker with the IC_{50} value given by $1/\varepsilon_{\mathrm{CaL}}$. Then the animal model in the setting when the drug has been applied is given by

$$\frac{dv}{dt} = -g_1 \mathrm{I}_{\mathrm{Na}} - \frac{g_2}{1 + D\varepsilon_{\mathrm{CaL}}} \mathrm{I}_{\mathrm{CaL}} - g_3 \mathrm{I}_{\mathrm{Ks}}, \tag{13}$$

where D denotes the concentration of the applied drug. Since the IC_{50} value of the single channel is the same for the animal and the human myocytes, the human model takes the form

Parameter	Human	Dog	Zebrafish	Rabbit	Guinea pig
g_{Kr} (mS/μF)	0.033	0.016	0.044	0.087	0.06
g_{CaL} (nL/(μF ms))	0.17	0.077	0.086	0.25	0.21
g_{Na} (mS/μF)	5	1.4	2.2	2.3	0.90
g_{Ks} (mS/μF)	0.003	0.1	0.0024	0.016	0.69
g_{KL} (mS/μF)	0.074	0.52	0.86	0.35	0.85
g_{to} (mS/μF)	0.54	0.31	0.0035	0.17	0.00
g_{NaL} (mS/μF)	0.025	0.0042	0.028	0.027	0.03
$\bar{I}_{NaCa}$ (μA/μF)	4.9	5.9	4.2	9.8	15.86
$\bar{I}_{NaK}$ (μA/μF)	1.8	1.4	9.2	2.8	1.62
g_{bCl} (mS/μF)	0.0056	0.00013	0.00087	0.011	0.00
g_{bCa} (mS/μF)	0.00055	0.00065	0.0019	0.0005	0.00
$\bar{I}_{pCa}$ (μA/μF)	0.068	0.58	0.056	0.064	0.60
g_{CaT} (mS/μF)	0	0	0.056	0	0

Table 4. Parameter values of the Base model used to represent different species. The remaining parameter values used in the simulations are as specified in[13].

$$\frac{dv}{dt} = -k_1 \mathrm{I}_{\mathrm{Na}} - \frac{k_2}{1 + D\varepsilon_{\mathrm{CaL}}} \mathrm{I}_{\mathrm{CaL}} - k_3 \mathrm{I}_{\mathrm{Kr}}.$$

This model can be used to compute chosen biomarkers of interest for the human action potential. In this particularly simple situation, we can conclude that:

1. One can use the animal datasets to reveal drug effect on human I_{Na} and $\mathrm{I}_{\mathrm{CaL}}$.
2. One cannot use the animal to get any information about human I_{Kr} because the animal does not have I_{Kr}.
3. The I_{Ks} current in the animal does not create difficulties for the measurements.

The base model of the action potential. In all of our simulations, we use the Base model derived in[13]. The parameters used to model human, dog, zebrafish, rabbit and guinea pig action potentials are given in Table 4. The remaining parameter values are specified in[13], except that the intracellular potassium concentration is increased from 120 mM to 145 mM for the dog case in order to match the resting potential observed in the data from[7]. Note also that because zebrafish cardiomyocytes have been shown to exhibit a robust T-type calcium current (I_{CaT})[17], the Base model from[13], when utilized for the zebrafish simulations, is extended to include a T-type calcium current from[53] of the form

$$I_{\mathrm{CaT}} = g_{\mathrm{CaT}} \cdot d \cdot f \cdot (v - E_{\mathrm{Ca}}),$$

where g_{CaT} is the conductance of the channels and E_{Ca} is the Nernst equilibrium potential for calcium (see[13]). Here, d and f are gating variables governed by

$$\frac{dd}{dt} = \frac{d_\infty - d}{\tau_d}, \quad d_\infty = \frac{1}{1 + e^{-(v+26.3)/6}},$$

$$\tau_d = \frac{1}{1.068e^{(v+26.3)/30} + 1.068e^{-(v+26.3)/30}},$$

$$\frac{df}{dt} = \frac{f_\infty - f}{\tau_f}, \quad f_\infty = \frac{1}{1 + e^{(v+61.7)/5.6}},$$

$$\tau_f = \frac{1}{0.0153e^{-(v+61.7)/83.3} + 0.015e^{(v+61.7)/15.38}}.$$

Inversion of data. The inversion of data from dog, zebrafish and rabbit action potentials is performed using the inversion procedure described in[13]. In the inversion, the adjustment factors λ_{Kr}, λ_{CaL}, λ_{Na}, λ_{Ks}, λ_{Kl}, λ_{to}, λ_{NaL}, λ_{NaCa}, λ_{NaK}, λ_{bCl}, λ_{bCa}, and λ_{pCa} for the currents I_{Kr}, I_{CaL}, I_{Na}, I_{Ks}, I_{Kl}, I_{to}, I_{NaL}, I_{NaCa}, I_{NaK}, I_{bCl}, I_{bCa}, and I_{pCa}, are treated as free parameters, in the zebrafish case, the adjustment factor λCaT for the current ICaT is also treated as a free parameter in the inversion, in addition to εKr (and $\varepsilon_{\mathrm{CaL}}$ for sotalol), representing the effect of the drug (see (6)).

Cost function definition. In the inversion, we minimize a cost function of the form

	Zebrafish control "measured"	Zebrafish drug "measured"	Human control "measured"	Human drug "measured"	Human control model	Human drug, estimated based on zebrafish data
APD50 (ms)	110	−7.9%	214	−10.5%	214	−9.3%
$\left(\frac{dv}{dt}\right)_{\max}$ (mV/ms)	102	−49.1%	195	−43.6%	195	−42.7%

Table 5. Effect of 50% block of I_{Na} and I_{CaL} on APD50 and the maximal upstroke velocity of the action potential in zebrafish and human models. The zebrafish and human data is generated from simulations of the zebrafish and human models specified in Section 5.2. In addition, the effect of the drug is estimated based on the zebrafish case and mapped to the human case in the rightmost column.

$$H(\lambda, \varepsilon) = \sum_d \sum_j w_{d,j}\left(H_j(\lambda, \varepsilon, D_d)\right)^2, \tag{14}$$

where d numbers the drug doses, D_d, included in the data set (including the control case), j numbers the different cost function terms, H_j, included in the cost function, and $w_{d,j}$ are specified weights for each of the cost function terms and each of the doses. The cost function includes the terms

$$H_{\mathrm{APD}p}(\lambda, \varepsilon, D_d) = \frac{|\mathrm{APD}p(\lambda, \varepsilon, D_d) - \mathrm{APD}p^*(D_d)|}{|\mathrm{APD}p^*(D_d)|}, \quad \text{for } p = 20, 30, \ldots, 90,$$

$$H_{v_{\max}}(\lambda, \varepsilon, D_d) = \frac{|v_{\max}(\lambda, \varepsilon, D_d) - v^*_{\max}(D_d)|}{|v^*_{\max}(D_d)|},$$

$$H_{v_{\min}}(\lambda, \varepsilon, D_d) = \frac{|v_{\min}(\lambda, \varepsilon, D_d) - v^*_{\min}(D_d)|}{|v^*_{\min}(D_d)|},$$

where APD p is the action potential duration at p percent repolarization (see[13]). Furthermore, $v_{\min}$ and $v_{\max}$ are the minimum and maximum values of the membrane potential, respectively. The terms marked by an * represent values computed from measured data, and the remaining terms are computed from simulations of the model defined by λ and ε.

Cost function weight. We use the weight 2 for $H_{v_{\max}}$, $H_{v_{\min}}$ and H_{APD50}, the weight 5 for H_{APD90} and the weight 1 for the remaining terms. In addition, the weights for the control case, $w_{0,j}$, are multiplied by the total number of doses included in the data set (including the control case).

Minimization procedure. In order to minimize the cost function (14), we apply the continuation-based minimization procedure from[13] using 10 iterations with 100 randomly chosen initial guesses. The initial guesses for λ are chosen within 10% above or below the optimal values from the previous iteration, and the initial guesses for ε_m are chosen within $[\varepsilon_{m-1}/5, 5\varepsilon_{m-1}]$, where ε_{m-1} is the optimal ε from the previous iteration. From these initial guesses we run 15 iterations of the Nelder-Mead algorithm[54]. The starting points for the first iteration of the continuation method are adjusted by hand.

Application of the method to generated data. In the main text, we have shown that we are able to use animal datasets (from dog, zebrafish and rabbit) to estimate the effect of I_{Kr} blockers on healthy human ventricular myocytes. However, available published data is limited and we therefore want to indicate that the methodology works more generally than we have been able to prove using available datasets. In Table 5, we have additionally used simulations to generate data. More specifically, we use the zebrafish model to estimate the effect for the human model of blocking the sodium current and the calcium current by 50%. In these inversions, λ_{Na}, λ_{CaL} and λ_{Kr} and ε_{Na}, ε_{CaL} and ε_{Kr} are treated as free parameters. In the generation of the zebrafish data, I_{Na}, I_{CaL} and I_{Kr} are all increased by 20%. Furthermore, in order to detect changes in the sodium current, we extend the cost function to include the term

$$H_{\mathrm{dvdt}}(\lambda, \varepsilon, D_d) = \frac{\left|\left|\frac{dv(\lambda, \varepsilon, D_d)}{dt}\right| - \left|\frac{dv^*(D_d)}{dt}\right|\right|}{\left|\left|\frac{dv^*(D_d)}{dt}\right|\right|},$$

measuring differences in the upstroke velocity. The results in Table 5 illustrate that the method presented here has wide applicability, provided that the ion currents under consideration have significant impact on both animal and human action potentials.

	Guinea pig control measured	Guinea pig drug measured	Zebrafish control measured	Zebrafish drug measured	Zebrafish control model	Zebrafish drug estimated based on guinea pig data
APD50 (ms)	156	+10.2% (1 nM)	108		111	+1.0% (1 nM)
		+16.4% (30 nM)				+17.8% (30 nM)
		+30.1% (100 nM)				+30.4% (100 nM)
		+37.2% (1 μM)		+38.7% (1 μM)		+41.7% (1 μM)
APD90 (ms)	178	+9.9% (1 nM)	133		133	+0.8% (1 nM)
		+16.6% (30 nM)				+15.0% (30 nM)
		+31.5% (100 nM)				+25.6% (100 nM)
		+38.4% (1 μM)		+35.4% (1 μM)		+35.2% (1 μM)

Table 6. APD values computed from measured and simulated action potentials in the control case and in the presence of the I_{Kr} blocker E-4031. The guinea pig data are from[18] and include the control case and the four drug doses 1 nM, 30 nM, 100 nM and 1 μM. The zebrafish data are from[17] and include the control case and the case of 1 μM E-4031[55].

Quantitative translation from guinea pig to zebrafish. The purpose of this paper is to show how a computational approach can be used to translate measured drug responses for animals to corresponding drug responses for humans. We have demonstrated how data from dogs, zebrafish and rabbits can be translated into predictions of human drug responses. In Table 6, we demonstrate how the same approach may be used to translate the effect of a drug from one animal to another. In this case, we consider data from[18] of guinea pig cardiomyocytes exposed to four different doses of the I_{Kr} blocker E-4031. In addition, measured zebrafish data of 1 μM E-4031 are provided in[17]. Based on the measured guinea pig data, the mathematical method estimates an IC_{50} value of 27 nM for block of I_{Kr} by E-4031. This is in good agreement with values found in literature (10–397 nM[25–30]) as well as with the IC_{50} value of 44 nM identified based on zebrafish data in the main text. In Table 6, we observe that the method predicts a 41.7% increase in APD50 and a 35.2% increase in APD90 for zebrafish cardiomyocytes exposed to 1 μM E-4031, in line with the measured increases of 38.7% and 35.4% for APD50 and APD90, respectively.

Received: 27 February 2020; Accepted: 26 May 2020;
Published online: 29 June 2020

References

1. Edwards, A. G. & Louch, W. E. Species-dependent mechanisms of cardiac arrhythmia: a cellular focus. *Clinical Medicine Insights: Cardiology*, **11**, 1179546816686061 (2017).
2. Yoshida, Y. & Yamanaka, S. Induced pluripotent stem cells 10 years later. *Circulation Research* **120**(12), 1958–1968 (2017).
3. Ye, L., Ni, X., Zhao, Z.-A., Lei, W. & Hu, S. The application of induced pluripotent stem cells in cardiac disease modeling and drug testing. *Journal of Cardiovascular Translational Research* **11**(5), 366–374 (2018).
4. DiMasi, J. A., Grabowski, H. G. & Hansen, R. W. Innovation in the pharmaceutical industry: New estimates of R&D costs. *Journal of Health Economics* **47**, 20–33 (2016).
5. Paul, S. M. *et al*. How to improve R&D productivity: the pharmaceutical industry's grand challenge. *Nature Reviews Drug Discovery* **9**(3), 203–214 (2010).
6. Bockorny, M., Chakravarty, S., Schulman, P., Bockorny, B. & Bona, R. Severe heart failure after bortezomib treatment in a patient with multiple myeloma: A case report and review of the literature. *Acta Haematologica* **128**(4), 244–247 (2012).
7. Jost, N. *et al*. Ionic mechanisms limiting cardiac repolarization reserve in humans compared to dogs. *The Journal of Physiology* **591**(17), 4189–4206 (2013).
8. Zicha, S. *et al*. Molecular basis of species-specific expression of repolarizing K+ currents in the heart. *American Journal of Physiology-Heart and Circulatory Physiology* **285**(4), H1641–H1649 (2003).
9. Wang, Z. *et al*. Potential molecular basis of different physiological properties of the transient outward K+ current in rabbit and human atrial myocytes. *Circulation Research* **84**(5), 551–561 (1999).
10. Gemmell, P., Burrage, K., Rodriguez, B. & Quinn, T. A. Population of computational rabbit-specific ventricular action potential models for investigating sources of variability in cellular repolarisation. *Plos One* **9**(2), e90112 (2014).
11. Grandi, E., Pasqualini, F. S. & Bers, D. M. A novel computational model of the human ventricular action potential and Ca transient. *Journal of Molecular and Cellular Cardiology* **48**(1), 112–121 (2010).
12. Tveito, A. *et al*. Inversion and computational maturation of drug response using human stem cell derived cardiomyocytes in microphysiological systems. *Scientific Reports* **8**(1), 17626 (2018).
13. Jaeger, K. H. *et al*. Improved computational identification of drug response using optical measurements of human stem cell derived cardiomyocytes in microphysiological systems. *Frontiers in Pharmacology* **10**, 1648 (2020).
14. Niederer, S. A., Fink, M., Noble, D. & Smith, N. P. A meta-analysis of cardiacelectrophysiology computational models. *Experimental Physiology*, **94**(5), 486–495, 5 (2009).
15. Groenendaal, W. *et al*. Cell-specific cardiac electrophysiology models. *Plos computational biology* **11**(4), e1004242 (2015).
16. Jaeger, K. H., Wall, S. & Tveito, A. Detecting undetectables: Can conductances of action potential models be changed without appreciable change in the transmembrane potential? *Chaos: An Interdisciplinary Journal of Nonlinear Science* **29**(7), 073102 (2019).
17. Nemtsas, P., Wettwer, E., Christ, T., Weidinger, G. & Ravens, U. Adult zebrafish heart as a model for human heart? An electrophysiological study. *Journal of Molecular and Cellular Cardiology* **48**(1), 161–171 (2010).
18. Bussek, A. *et al*. Tissue slices from adult mammalian hearts as a model for pharmacological drug testing. *Cellular Physiology and Biochemistry* **24**(5-6), 527–536 (2009).
19. Jost, N. *et al*. Restricting excessive cardiac action potential and QT prolongation: a vital role for IKs in human ventricular muscle. *Circulation* **112**(10), 1392–1399 (2005).

20. Baczkó, I., Jost, N., Virág, L., Bösze, Z. & Varró, A. Rabbit models as tools for preclinical cardiac electrophysiological safety testing: importance of repolarization reserve. *Progress in Biophysics and Molecular Biology* **121**(2), 157–168 (2016).
21. Orvos, P. *et al*. Evaluation of possible proarrhythmic potency: Comparison of the effect of dofetilide, cisapride, sotalol, terfenadine, and verapamil on hERG and native IKr currents and on cardiac action potential. *Toxicological Sciences* **168**(2), 365–380 (2019).
22. Crumb, W. J., Vicente, J., Johannesen, L. & Strauss, D. G. An evaluation of 30 clinical drugs against the comprehensive *in vitro* proarrhythmia assay (CiPA) proposed ion channel panel. *Journal of Pharmacological and Toxicological Methods*, **81**:251–262 Focused Issue on Safety Pharmacology (2016).
23. Kramer, J. *et al*. MICE models: superior to the HERG model in predicting Torsade de Pointes. *Scientific Reports* **3**, 2100 (2013).
24. Qu, Y. & Vargas, H. M. Proarrhythmia risk assessment in human induced pluripotent stem cell-derived cardiomyocytes using the maestro MEA platform. *Toxicological Sciences* **147**(1), 286–295 (2015).
25. Kim, K.-S. & Kim, E.-J. The phenothiazine drugs inhibit hERG potassium channels. *Drug and Chemical Toxicology* **28**(3), 303–313 (2005).
26. Gibson, J. K., Yue, Y., Bronson, J., Palmer, C. & Numann, R. Human stem cell-derived cardiomyocytes detect drug-mediated changes in action potentials and ion currents. *Journal of Pharmacological and Toxicological Methods* **70**(3), 255–267 (2014).
27. Katayama, Y. *et al* The inter-cell-line reproducibility of hERG assay using the whole-cell patch-clamping. *Journal of Pharmacological Sciences*, **97** (2005).
28. McPate, M. J., Duncan, R. S., Witchel, H. J. & Hancox, J. C. Disopyramide is an effective inhibitor of mutant HERG K^+ channels involved in variant 1 short QT syndrome. *Journal of Molecular and Cellular Cardiology* **41**(3), 563–566 (2006).
29. Piper, D. R. *et al*. Development of the predictor HERG uorescence polarization assay using a membrane protein enrichment approach. *Assay and Drug Development Technologies* **6**(2), 213–223 (2008).
30. Sanguinetti, M. C. & Jurkiewicz, N. K. Two components of cardiac delayed rectifier K^+ current. differential sensitivity to block by class III antiarrhythmic agents. *The Journal of General Physiology* **96**(1), 195–215 (1990).
31. Shanks, N., Greek, R. & Greek, J. Are animal models predictive for humans? *Philosophy, Ethics, and Humanities in Medicine* **4**(1), 2 (2009).
32. Hill, A. J. & Iaizzo, P. A. Comparative cardiac anatomy. In *Handbook of cardiac anatomy, physiology, and devices*, pages 89–114. Springer (2015).
33. Houser, S. R. *et al*. Animal models of heart failure: a scientific statement from the American Heart Association. *Circulation Research* **111**(1), 131–150 (2012).
34. Gong, J. Q. X. & Sobie, E. A. Population-based mechanistic modeling allows for quantitative predictions of drug responses across cell types. *NPJ Systems Biology and Applications* **4**(1), 11 (2018).
35. Bailey, J., Thew, M. & Balls, M. An analysis of the use of dogs in predicting human toxicology and drug safety. *Alternatives to Laboratory Animals* **41**(5), 335–350 (2013).
36. Ando, K. *et al*. QT PRODACT: *In vivo* QT assay with a conscious monkey for assessment of the potential for drug-induced QT interval prolongation. *Journal of pharmacological sciences* **99**(5), 487–500 (2005).
37. Bergenholm, L., Collins, T., Evans, N. D., Chappell, M. J. & Parkinson, J. PKPD modelling of PR and QRS intervals in conscious dogs using standard safety pharmacology data. *Journal of Pharmacological and Toxicological Methods* **79**, 34–44 (2016).
38. Bergenholm, L. *et al*. Predicting QRS and PR interval prolongations in humans using nonclinical data. *British Journal of Pharmacology* **174**(19), 3268–3283 (2017).
39. Jegla, T. J., Zmasek, C. M., Batalov, S. & Nayak, S. K. Evolution of the human ion channel set. *Combinatorial Chemistry & High Throughput Screening* (2009).
40. Jost, N. *et al*. A kesoi egyeniranyito kaliumaram gyors (IKr) es lassu komponensenek (IKs) osszehasonlito vizsgalata egeszseges emberi, kutya, nyul es tengerimalac kamrai szivizomsejteken. *Cardiologia Hungarica* **34**, 103–113 (2004).
41. Blechschmidt, S., Haufe, V., Benndorf, K. & Zimmer, T. Voltage-gated Na+ channel transcript patterns in the mammalian heart are speciesdependent. *Progress in Biophysics and Molecular Biology* (2008).
42. Zimmer, T., Haufe, V. & Blechschmidt, S. Voltage-gated sodium channels in the mammalian heart. *Global Cardiology Science and Practice* (2014).
43. Rudy, Y. From genes and molecules to organs and organisms: Heart. *Comprehensive Biophysics*, pages 268–327 (2012).
44. Rudy, Y. & Silva, J. R. Computational biology in the study of cardiac ion channels and cell electrophysiology. *Quarterly Reviews of Biophysics* **39**(01), 57–116 (2006).
45. Plonsey, R. & Barr, R. C. Bioelectricity, A Quantitative Approach. *Springer* (2007).
46. Sterratt, D., Graham, B., Gillies, A. & Willshaw, D. Principles of Computational Modelling in Neuroscience. *Cambridge University Press* (2011).
47. Tveito, A. & Lines, G. T. Computing Characterizations of Drugs for Ion Channels and Receptors Using Markov Models. *Springer-Verlag, Lecture Notes*, vol. 111 (2016).
48. Brennan, T., Fink, M. & Rodriguez, B. Multiscale modelling of drug-induced effects on cardiac electrophysiological activity. *EuropeanJournal of Pharmaceutical Sciences* **36**(1), 62–77 (2009).
49. Clancy, C. E., Zhu, Z. I. & Rudy, Y. Pharmacogenetics and anti-arrhythmic drug therapy: A theoretical investigation. *AJP: Heart and Circulatory Physiology* **292**(1), H66–H75 (2007).
50. Tveito, A., Maleckar, M. M. & Lines, G. T. Computing optimal properties of drugs using mathematical models of single channel dynamics. Computational and Mathematical. *Biophysics* **6**(1), 41–64 (2018).
51. Kernik, D. C. *et al*. A computational model of inducedpluripotent stem-cell derived cardiomyocytes incorporating experimental variability from multiple data sources. *The Journal of Physiology* (2019).
52. O'Hara, T., Virág, L., Varró, A. & Rudy, Y. Simulation of the undiseasedhuman cardiac ventricular action potential: Model formulation and experimental validation. *PLoS Computational Biology* **7**(5), e1002061 (2011).
53. Maltsev, V. A. & Lakatta, E. G. Synergism of coupled subsarcolemmalCa^{2+} clocks and sarcolemmal voltage clocks confers robust and exible pacemaker function in a novel pacemaker cell model. *American Journal of Physiology-Heart and Circulatory Physiology* **296**(3), H594–H615 (2009).
54. Nelder, J. A. & Mead, R. A simplex method for function minimization. *The Computer Journal* **7**(4), 308–313 (1965).
55. Carlsson, L. *In vitro* and *in vivo* models for testing arrhythmogenesis in drugs. *Journal of Internal Medicine* **259**(1), 70–80 (2006).

Author contributions

A.T. and K.H.J. did the mathematical modeling, performed numerical simulations, and wrote the paper; M.M.M., W.R.G. and S.W. reviewed the paper as a whole, and provided editing concerning relevance to existing literature on animal models (W.R.G.), relevance to drug development (S.W.), and applicability of the mathematical model (M.M.M.).

Competing interests

The authors declare no competing interests.

Additional information

Correspondence and requests for materials should be addressed to A.T.

Reprints and permissions information is available at www.nature.com/reprints.

Publisher's note Springer Nature remains neutral with regard to jurisdictional claims in published maps and institutional affiliations.